Study of A-site ordered PrBaMn$_2$O$_{6-\delta}$ manganite properties depending on the treatment conditions

Study of A-site ordered $PrBaMn_2O_{6-\delta}$ manganite properties depending on the treatment conditions

S V Trukhanov[1]**, L S Lobanovski**[1]**, M V Bushinsky**[1]**, V V Fedotova**[1]**, I O Troyanchuk**[1]**, A V Trukhanov**[2]**, V A Ryzhov**[3]**, H Szymczak**[4]**, R Szymczak**[4] **and M Baran**[4]

[1] Institute of Solids and Semiconductor Physics of NASB, P Brovka Street 17, 220072 Minsk, Belarus
[2] Chemistry Department, Vitebsk State University, Moscow Avenue 33, 210036 Vitebsk, Belarus
[3] Petersburg Nuclear Physics Institute RAS, Gatchina, St Petersburg 188300, Russian Federation
[4] Institute of Physics, PAS, Lotnikov street 32/46, 02-668 Warsaw, Poland

E-mail: truhanov@ifttp.bas-net.by and szymh@ifpan.edu.pl

Abstract
The effect of treatment conditions on the magnetic and magnetotransport properties of A-site ordered $PrBaMn_2O_{6-\delta}$ manganites is examined. The parent oxygen-stoichiometric A-site ordered $PrBaMn_2O_6$ samples were prepared from oxygen-stoichiometric A-site disordered $Pr_{0.50}Ba_{0.50}MnO_3$ ones by using a 'two-step' synthesis method. The most significant structural feature of the A-site ordered manganites is that the MnO_2 sublattice is sandwiched by two kinds of rock-salt layers, PrO_x and BaO. The oxygen-stoichiometric A-site ordered $PrBaMn_2O_6$ demonstrates a ferromagnetic metal to paramagnetic insulator transition with the Curie point at about 320 K. These compounds are stable in air up to 1300 °C. The A-site ordered $PrBaMn_2O_6$ samples were next reduced in flowing argon as well as being treated under high pressure conditions. The reduction of the A-site ordered $PrBaMn_2O_6$ samples leads to the appearance of an antiferromagnetic state with a Néel point of about 140 K, while the A-site order remains. Upon high pressure treatment the degree of A-site order decreases, which reduces T_C to 180 K. The magnetotransport properties of A-site ordered manganites treated under different conditions are discussed in terms of the manganese valence, oxygen content and degree of A-site order.

1. Introduction

The perovskite-type manganites $Ln_{1-x}A_xMnO_3$ ($Ln = La$, Nd, Pr etc, $A = Ca$, Sr, Ba etc) have been intensively investigated experimentally and theoretically due to their very large negative magnetoresistance (MR) near their Curie temperatures and the intriguing physics caused by the

strong interplay between the lattice, charge and spin degrees of freedom [1]. The large negative MR observed for the perovskite manganites is now termed 'colossal magnetoresistance' (CMR) to distinguish it from the giant magnetoresistance (GMR) observed in transition metal systems in multilayer or granular forms. CMR has been observed in hole-doped $Pr_{1-x}Ca_xMnO_3$ manganites, for example [2].

The parent compound for all the doped manganites is $LaMnO_3$ antiferromagnetic insulator, which involves Mn^{3+} ions with the $t_{2g}^3e_g^1(S = 2)$ configuration. In this compound all the Mn^{3+} ions are surrounded by oxygen octahedra. The Hund-coupled t_{2g}^3 electrons are localized and may be viewed as a single local spin ($S = 3/2$) because of their narrow one-electron bandwidth, and the e_g^1 electron is hybridized strongly with the O 2p orbital and may be viewed as localized in this substance. However, it was suggested that hole doping with divalent alkaline-earth A^{2+} ions can lead for trivalent rare-earth Ln^{3+} ions to both metallic conductivity and ferromagnetism in the $Ln_{1-x}^{3+}A_x^{2+}Mn_{1-x}^{3+}Mn_x^{4+}O_3^{2-}$ compounds. In this case Mn^{4+} ions are created from Mn^{3+}. The Mn^{4+} ion contains t_{2g}^3 state electrons only, which are localized [3]. A Zener double-exchange (DE) interaction has been proposed as the cause of the metallic behaviour and of the strong ferromagnetic interactions between Mn^{3+} and Mn^{4+} ions. The main role in the DE interaction is played by the mixed valence of the manganese ions, with the hopping of e_g electrons between Mn^{3+} and Mn^{4+} mediated by the oxygen anions [4].

The understanding of the CMR phenomenon, metallic behaviour and strong ferromagnetic interactions between Mn ions requires a systematic study of the relationships between the magnetic and electrical properties and the crystal structure of the manganese oxide perovskites. In this respect, the $Ln_{0.50}A_{0.50}MnO_3$ (Ln = La, Pr, Nd; A = Ca, Sr, Ba) perovskites are of great interest, considering that these phases exhibit both antiferromagnet–ferromagnet and charge order–disorder transitions [5–7] except for Ba-doped samples.

For example, in the Ca series only $La_{0.50}Ca_{0.50}MnO_3$ is a ferromagnetic semiconductor ($T_C = 225$ K) and it transforms to the charge ordered antiferromagnetic semiconductor (CE-type) phase through an incommensurate ferromagnetic semiconductor phase. $Pr_{0.50}Ca_{0.50}MnO_3$ and $Nd_{0.50}Ca_{0.50}MnO_3$ are paramagnetic semiconductors above T_N and transform directly to charge ordered antiferromagnetic (CE-type) ones through a charge ordered paramagnetic semiconductor phase. The critical temperature of the charge ordering (T_{CO}) is well above the Néel temperature T_N and the two transitions are clearly decoupled [8].

For the $La_{0.50}Sr_{0.50}MnO_3$ sample the ferromagnetic state ($T_C = 360$ K) is stable down to 200 K. $Pr_{0.50}Sr_{0.50}MnO_3$ undergoes a transition from the ferromagnetic metal ($T_C = 275$ K) to the antiferromagnetic (A-type) semiconductor state and $Nd_{0.50}Sr_{0.50}MnO_3$ with $T_C = 255$ K becomes antiferromagnetic (CE-type).

The $Ln_{0.50}Ba_{0.50}MnO_3$ manganites are much less well studied. It has been revealed that they do not show antiferromagnet–ferromagnet and charge order–disorder transitions [9]. It is known that $La_{0.50}Ba_{0.50}MnO_3$ is a ferromagnet with $T_C \approx 270$ K [10]. $Pr_{0.50}Ba_{0.50}MnO_3$ and $Nd_{0.50}Ba_{0.50}MnO_3$ have Curie points of 140 K [11] and 80 K [9], respectively. In another respect, Ba-doped manganites should be of interest: due to the high mismatch between lanthanide and Ba ionic sizes. The difference between lanthanide and alkaline-earth ionic radii strongly reduces T_C [12].

Recently, it has been reported that the magnetotransport properties of the $Ln_{0.50}Ba_{0.50}MnO_3$ manganites strongly depend on the arrangement of the Ln^{3+} and Ba^{2+} ions in the A sublattice of the perovskite structure [10, 11, 13–25]. It has been shown that the A-site ordered compounds may be synthesized by the topotactic reduction–oxidation method. Structural investigations have shown the oxygen-stoichiometric $LnBaMn_2O_6$ compounds obtained in air to be cubic with disordered Ln^{3+} and Ba^{2+} cations, whereas the oxygen-deficient

LnBaMn$_2$O$_5$ compounds are tetragonal with ordered Ln^{3+} and Ba^{2+} cations and an alternating stacking of rare-earth and barium containing layers along the direction c. This crystal structure of the oxygen-deficient LnBaMn$_2$O$_5$ compounds is similar to that of the related compound YBaCuFeO$_5$. Another form of oxygen-stoichiometric LnBaMn$_2$O$_6$ compound obtained by the reoxidation of oxygen-deficient LnBaMn$_2$O$_5$ is also tetragonal and retains the ordering of Ln^{3+} and Ba^{2+} cations. It is observed that this type of cation ordering leads to considerable increase of the temperature of transition to the paramagnetic insulating state. The A-site disordered Pr$_{0.50}$Ba$_{0.50}$MnO$_3$ compound is ferromagnetic with $T_C \approx 140$ K while A-site ordered PrBaMn$_2$O$_6$ has $T_C \approx 320$ K. The electrical resistivity behaviour correlates with the magnetization. Below T_C this compound undergoes a transition to a metallic state and demonstrates a peak of magnetoresistance of about 10% in a field of 9 kOe [14].

It has also been shown that the Ba-doped compounds may have various degrees of Pr/Ba randomness at the A sites. The A-site disorder gradually suppresses both the ferromagnetic and A-type antiferromagnetic transitions and finally leads to a magnetic glassy state for the Pr$_{0.50}$Ba$_{0.50}$MnO$_3$ [20]. These results show that the oxygen deficiency and the ordering of oxygen vacancies are closely related to the ordering of lanthanum and barium in the structure.

Recently [21] it has been demonstrated that annealing LnBaMn$_2$O$_6$ under O$_2$ gas at high temperatures always resulted in insufficient Ln/Ba solid solution at the A sites. Pr–Ba compounds with various degrees of A-site order have been synthesized from PrBaMn$_2$O$_6$ by controlling the annealing time and temperatures (1273–1623 K) in O$_2$ gas. The sample with 96% (PB96) A-site order was obtained by heating the starting Pr$_{0.50}$Ba$_{0.50}$MnO$_3$ material at 1623 K in pure Ar for 24 h and then annealing it at 1623 K in O$_2$ for 24 h. The sample with 87% A-site order was obtained by annealing PB96 at 1273 K in O$_2$ for 6 h. The sample with 0% A-site order was obtained by heating the starting Pr$_{0.50}$Ba$_{0.50}$MnO$_3$ material at 1623 K in 1% O$_2$/Ar for 24 h and then annealing it at 1173 K in O$_2$ for 24 h.

Thus it is of interest to study the magnetotransport properties of the A-site ordered PrBaMn$_2$O$_{6-\delta}$ systems that depend on both the A-site degree of order and the oxygen content. The preparation conditions and magnetotransport properties for the A-site ordered PrBaMn$_2$O$_5$ and PrBaMn$_2$O$_6$ were reported earlier, by us [14]. In the present paper, we report the preparation conditions, magnetization, electrical resistivity and magnetoresistance properties of A-site ordered PrBaMn$_2$O$_{6-\delta}$ samples as a function of oxygen content and degree of A-site order.

2. Experimental method

The starting material, A-site ordered PrBaMn$_2$O$_6$, was obtained from high purity oxides and carbonate: Pr$_2$O$_3$, Mn$_2$O$_3$ and BaCO$_3$, using a 'two-step' topotactic reduction–oxidation method [14]. First the oxides and carbonate were mixed in the desired ratio. Then the prefiring was performed at 1000 °C in air for 1 h. Final synthesis was carried out at 1550 °C in air for 2 h. After synthesis the samples were slowly cooled (100 °C h^{-1}) in order to take in the stoichiometric oxygen content. The air-prepared Pr$_{0.50}$Ba$_{0.50}$MnO$_3$ samples were treated in an evacuated silica tube at 800 °C for 24 h, using Ta as the oxygen getter, down to the 'O$_{2.50}$' phase:

$$Pr_{0.5}Ba_{0.5}MnO_3 + 0.2Ta \rightarrow Pr_{0.5}Ba_{0.5}MnO_{2.50} + 0.1Ta_2O_5. \qquad (1)$$

As we will see below, the 'O$_{2.50}$' phase is characterized by the ordered Pr^{3+} and Ba^{2+} ion location and alternating stacking of praseodymium and barium containing layers along c. As a result of the ordered location of the A ions the unit cell of the 'O$_{2.50}$' phase is doubled and we will term it A-site ordered 'O$_5$'. The A-site ordered PrBaMn$_2$O$_5$ samples were oxidized in

Table 1. The oxygen content and degree of A-site order for all of the $PrBaMn_2O_{6-\delta}$ samples after exposure to extreme conditions.

	Chemical formula	Conditions of treatment	Oxygen content	Degree of A-site order (%)	Sample marking
1.	$Pr_{0.50}Ba_{0.50}MnO_{3.00}$	As-prepared Synthesized in air, 1550 °C	3.00	0	O30A00
2.	$PrBaMn_2O_{6.00}$	Annealed in air, 800 °C	6.00	100	O60A100
3.	$PrBaMn_2O_{6.00}$	Annealed in air, 1100 °C	6.00	70	O60A70
4.	$PrBaMn_2O_{6.00}$	Annealed in air, 1200 °C	6.00	50	O60A50
5.	$PrBaMn_2O_{6.00}$	Annealed in air, 1300 °C	6.00	0	O60A00
6.	$PrBaMn_2O_{5.90}$	Annealed in Ar, 600 °C	5.90	100	O59A100
7.	$PrBaMn_2O_{5.60}$	Annealed in Ar, 800 °C	5.60	100	O56A100
8.	$PrBaMn_2O_{6.00}$	Under high pressure	6.00	25	O60A25

air at 800 °C for 5 h up to the A-site ordered 'O$_6$' phase:

$$PrBaMn_2O_5 + O_2 \rightarrow PrBaMn_2O_6. \tag{2}$$

Then the oxygen-stoichiometric A-site ordered $PrBaMn_2O_6$ samples were treated in extreme conditions: (1) in flowing argon at 600 and 800 °C for 5 h down to the A-site ordered 'O$_{5.90}$' and 'O$_{5.60}$' phases; (2) under high pressure conditions ($P = 6$ GPa, $T = 600$ °C); as well as (3) in air at 1100, 1200 and 1300 °C for 10 h. Upon high pressure treatment and air annealing, the oxygen stoichiometry does not change.

The chemical content of all the samples was investigated by electronic Auger spectroscopy with an electronic scanning Auger spectrometer, PHI-660 (Scanning Auger Multiprobe). The oxygen content of the final products was determined by a thermogravimetric (TG) method involving reduction in an H_2/N_2 flow at 600 °C. The chemical formula for the samples examined may be written as $Pr_{0.50}Ba_{0.50}MnO_{3-\gamma\pm0.01}$ for the A-site disordered 'O$_{3-\gamma}$' phase and $PrBaMn_2O_{6-\delta\pm0.02}$ for the A-site ordered 'O$_{6-\delta}$' one. The Mn valence for all the samples was determined by redox potentiometric titration using potassium dichromate and ferrous ammonium sulfate. The microstructure of all the samples obtained was studied using a NANOLAB-7 scanning electron microscope. The quantitative chemical content and its spatial distribution were examined by using MS-46 and SYSTEM-860-500 microprobes. These investigations showed that all the samples obtained are well crystallized with homogeneous chemical content. X-ray powder diffraction data were recorded at room temperature with a DRON-3 diffractometer with Cr Kα radiation.

The degree of A-site order (A) for all the $[Pr_gBa_{1-g}]_P[Pr_{1-g}Ba_g]_BMn_2O_{6-\delta}$ samples obtained was determined from the powder x-ray data by considering the (0 0 1/2) peak intensity, according to the relation

$$A = (2g - 1) \times 100\% \tag{3}$$

where [ ]$_P$ and [ ]$_B$ represent the Pr and Ba sites in $PrBaMn_2O_{6-\delta}$, respectively. The g value varies from 0.5 for fully disordered ($A = 0\%$) to 1 for fully ordered ($A = 100\%$) systems. The oxygen stoichiometry and degree of A-site order for all the samples after exposure to extreme conditions are given in table 1, which also gives the sample labelling.

The magnetization measurements were made using an OI-3001 vibrating sample magnetometer. The dynamic magnetic susceptibility was measured with a mutual inductance bridge. The frequency of the field was equal to 1200 Hz. The magnetic ordering temperature (T_{MO}) was defined as the point where the magnetic susceptibility value becomes less than 10% of the total one. The value of the spontaneous magnetization (M_S) was determined from the
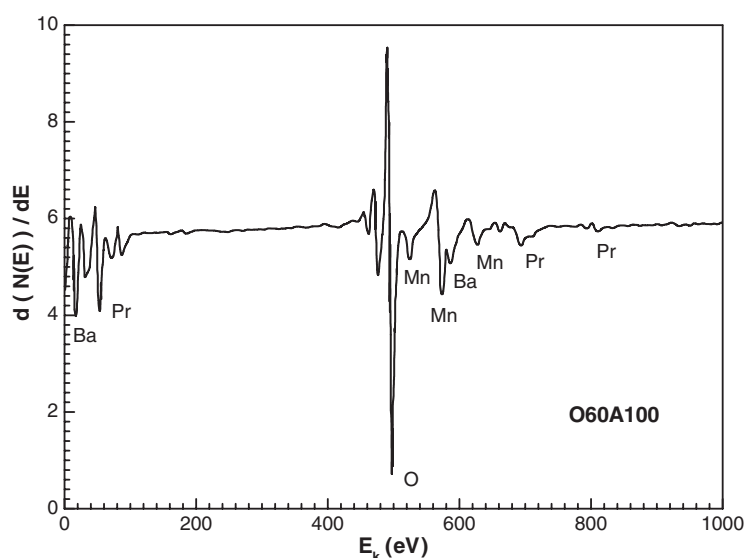
Figure 1. The differential Auger spectrum for the A-site ordered PrBaMn$_2$O$_6$ (O60A100) sample.

field dependence of the magnetization, by extrapolation to zero field. The dc resistivity of the samples was measured by the standard four-probe technique over the temperature range 77–350 K. Eutectic indium was employed for forming the contacts. The magnetoresistivity was calculated according to the relation

$$\text{MR} = \{[\rho(H) - \rho(H = 0)]/\rho(H = 0)\} \times 100\% \tag{4}$$

where MR is the negative isotropic magnetoresistance, $\rho(H)$ is the resistivity in a magnetic field of 9 kOe, $\rho(H = 0)$ is the resistivity without a magnetic field.

3. Results and discussion

The main aim of this work was obtaining A-site ordered PrBaMn$_2$O$_{6-\delta}$ samples and studying their properties as a function of the oxygen content and degree of A-site order. The reduction of these samples was performed by a topotactic method that does not involve any changes of the perovskite structure of the parent sample. First, the samples obtained were investigated as regards stoichiometry and homogeneity of the chemical content by an electronic Auger-spectroscopy method. The differential Auger spectrum for the A-site ordered PrBaMn$_2$O$_6$ (O60A100) sample is presented in figure 1. Quantitative evaluation has shown that the samples contain only Pr, Ba, Mn and O elements in the projected ratio. Impurity elements were not revealed. The cation ratio was Pr:Ba:Mn = 1:1:2. The cation distribution was homogeneous.

From the scanning electron microscopy observations, well cristated microstructure was found for the A-site ordered samples after the 'two-step' procedure. All the treatment conditions which can definitely affect the morphology of the ceramic obtained were identical. Keeping all the synthesis parameters the same for all the samples, similar microstructures were obtained. The average grain size for the samples is ∼200 nm. Upon heat treatment, the grain size was found to be invariant while temperature increases.

Most hole-doped perovskite manganites show lattice distortions as modifications from the cubic structure. One of the distortions is the deformation of the MnO$_6$ octahedron arising from the Jahn–Teller effect, peculiar to the high spin ($S = 2$) Mn^{3+} ions. Another comes from the
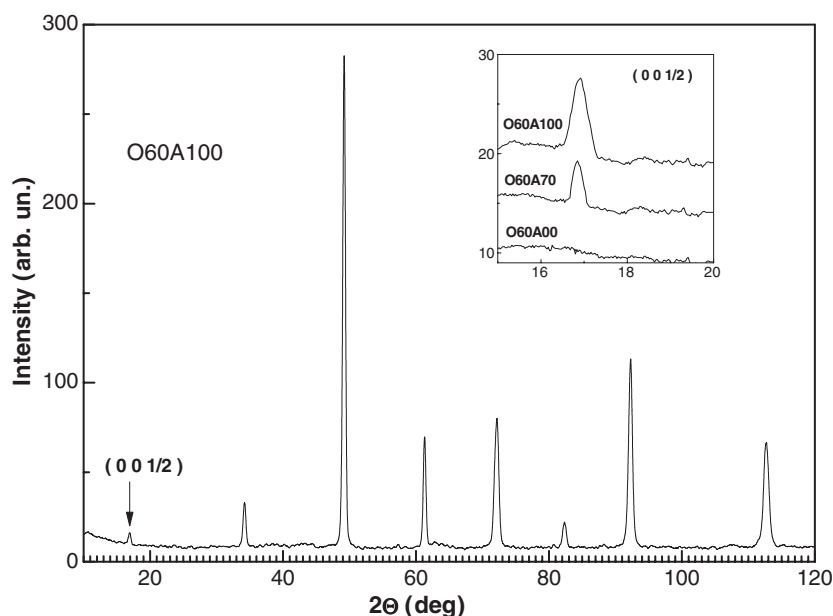
Figure 2. The powder x-ray diffraction pattern at room temperature for the A-site ordered $PrBaMn_2O_6$ (O60A100) sample. The inset shows the (0 0 1/2) reflection for samples with various degrees of A-site order: O60A00, O60A70 and O60A100.

size effect arising from the mismatch between the sizes of ions and the interstices occupied by them in the perovskite lattice. In this case, the MnO_6 octahedron is rotated around the cubic axes with the lattice symmetry lowering from cubic. The rotation around the [100] axis corresponds to tetragonal distortions, that around [110] to orthorhombic ones and that around [111] to rhombohedral ones.

According to our x-ray data the as-prepared $Pr_{0.50}Ba_{0.50}MnO_3$ (O30A00) sample is cubic (space group $Pm\bar{3}m$) at room temperature (figure 2). The unit cell parameter for the as-prepared $Pr_{0.50}Ba_{0.50}MnO_3$ (O30A00) sample is $a = 3.893$ Å ($V = 59.0$ Å^3). There is no extra peak suggesting a superstructure. All the reduced and reoxidized samples showed tetragonal (space group $P4/mmm$) distortions. The cubic symmetry is in agreement with the complete disordering of Pr^{3+} and Ba^{2+} ions on the A site of the perovskite cell. Parameter c for the tetragonally distorted samples doubles due to the ordering of the Pr^{3+} and Ba^{2+} ions. Direct evidence of the A-site ordering for all the reduced and reoxidized samples is provided from XRD data by the (0 0 1/2) reflection. The considerable changes of the crystal lattice allow us to examine all the tetragonal samples as ones with a doubled chemical formula, $PrBaMn_2O_{6-\delta}$.

An interesting feature is observed: the smaller the oxygen content, the larger the distortion and the volume of the unit cell. The unit cell for the reduced samples is greater than that for the oxidized samples, apparently due to conversion of the small Mn^{4+} ions into relatively large Mn^{3+} ions. The effective ionic radii of the Mn^{3+} and Mn^{4+} ions in octahedral oxygen coordination are 0.645 and 0.540 Å, respectively [26].

Nominally, the ratio of Mn^{3+} and Mn^{4+} ions is determined by the formula $Pr_{1-x}^{3+}Ba_x^{2+}Mn_{1-x}^{3+}Mn_x^{4+}O_3^{2-}$. But one can be slightly misled by assuming the Mn^{4+} content to be dictated simply by this formula, since it can vary with the methods and conditions of preparation. Therefore, careful investigation of the composition of the samples obtained
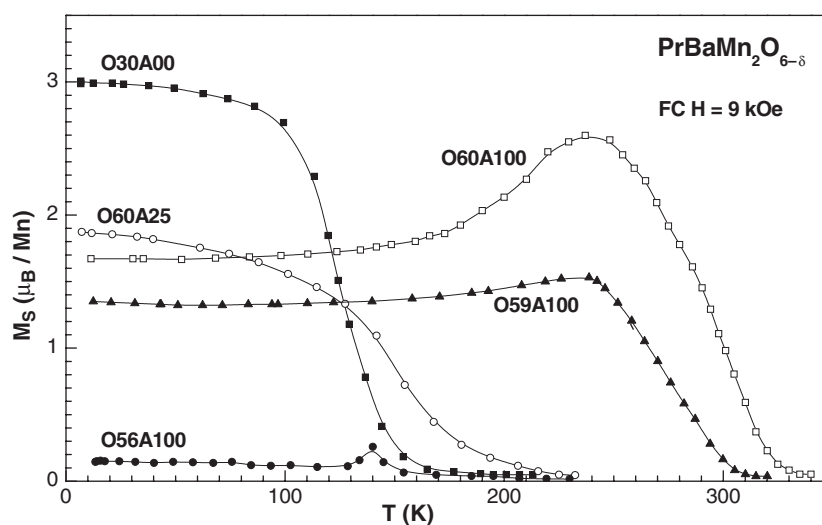
Figure 3. The temperature dependence of the FC (field cooled) magnetic moment in a field of 9 kOe for the PrBaMn$_2$O$_{6-\delta}$ samples: O30A00 (full rectangles), O60A100 (open rectangles), O59A100 (full triangles), O56A100 (full circles) and O60A25 (open circles).

by chemical analysis is needed. Redox potentiometric titration has shown that the average manganese valence corresponds to the formula $Pr_{0.50}^{3+}Ba_{0.50}^{2+}Mn_{0.50}^{3+}Mn_{0.50}^{4+}O_3^{2-}$.

The degree of A-site order for all the samples obtained was determined from the powder x-ray data considering the (0 0 1/2) superstructure peak intensity. The (0 0 1/2) reflection relates to the parent cubic unit cell. It is placed around $2\theta \sim 17°$ and ensures A-site modulation along the c axis. The intensity of the (0 0 1/2) reflection for the oxygen-stoichiometric PrBaMn$_2$O$_6$ (O60A100) sample reoxidized in air at 800 °C from PrBaMn$_2$O$_5$ was maximum and the degree of A-site order was taken as $A = 100\%$. The (0 0 1/2) intensity decreases with increasing A-site randomness and finally becomes undetectable for oxygen-stoichiometric PrBaMn$_2$O$_6$ (O60A00) annealed in air at 1300 °C for 10 h (inset of figure 2). The most significant structural feature of the A-site ordered manganites is that the MnO$_2$ sublattice is sandwiched by two kinds of rock-salt layers, PrO$_x$ and BaO.

The temperature dependence of the spontaneous magnetization for the samples prepared under different conditions is shown in figure 3. The as-prepared Pr$_{0.50}$Ba$_{0.50}$MnO$_3$ (O30A00) sample exhibits a transition into a paramagnetic state around $T_C = 140$ K. The magnetic moment per formula unit is $\sim$3 μ_B at 5 K in a field of 9 kOe, whereas the value expected for ferromagnetic ordering of all the magnetic moments of manganese ions is 3.5 μ_B per Mn (μ_B/Mn). It is well known that the magnetic moments for the manganese ions are $\mu(Mn^{3+}) = 4$ μ_B and $\mu(Mn^{4+}) = 3$ μ_B. For the PrBaMn$_2$O$_6$ (O60A100) sample annealed in air at 800 °C, the Curie point sharply increases to 320 K. This sample exhibits a peak of magnetization around 237 K. In this range of temperatures the hysteresis reaches 10 K, thus indicating a first-order phase transition. The maximum magnetic moment is 2.6 μ_B per Mn for this sample [11]. At 5 K the magnetic moment is 2.6 μ_B per Mn. The PrBaMn$_2$O$_{5.90}$ (O59A100) sample processed in flowing argon at 600 °C is an inhomogeneous ferromagnet with T_C being about 300 K. It also shows anomalous behaviour of the magnetization around 230 K, which is temperature hysteresis. 1.5 μ_B per Mn was revealed around 240 K. These data confirm the result obtained earlier that some intriguing properties can also be found upon reduction of the perovskite manganites [27]. The PrBaMn$_2$O$_{5.60}$ (O56A100) sample shows
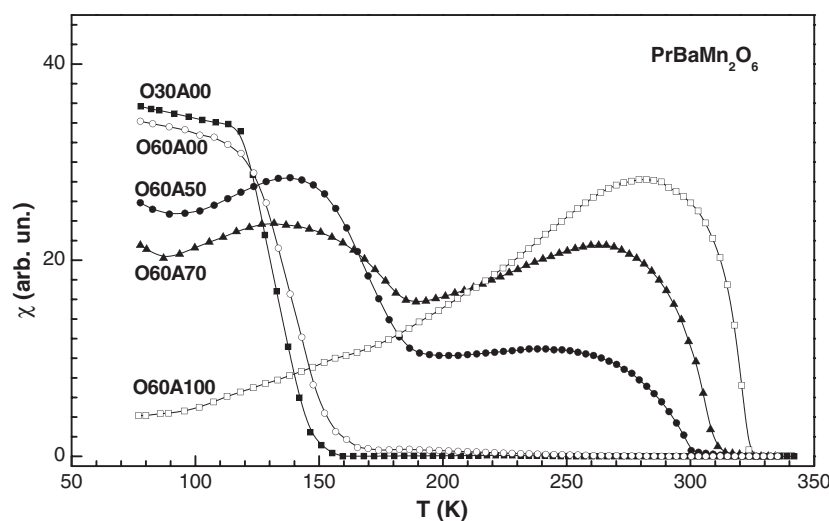
Figure 4. The temperature dependence of the ac susceptibility for the $PrBaMn_2O_6$ samples: O30A00 (full rectangles), O60A100 (open rectangles), O60A70 (full triangles), O60A50 (full circles) and O60A00 (open circles).

a weak magnetic moment equal to $\sim$0.1 μ_B/Mn at liquid helium temperature (figure 3). For this sample, near $T = 140$ K the magnetization has a visible peak and then it disappears. The treatment under pressure of $PrBaMn_2O_6$ (O60A100) leads to a decrease of the Curie point and the appearance of ferromagnetic properties only below $T_C = 180$ K. The maximum magnetic moment for the $PrBaMn_2O_6$ (O60A25) sample is $\sim$1.9 μ_B/Mn at liquid helium temperature.

As we have revealed, the A-site ordered $PrBaMn_2O_6$ (O60A100) sample is very stable in air up to 1300 °C. Figure 4 presents χ versus temperature for A-site disordered $Pr_{0.50}Ba_{0.50}MnO_3$ (O30A00) as well as A-site ordered $PrBaMn_2O_6$ (O60A100, O60A70, O60A50 and O60A00) samples. Each curve is $\chi(T)$ after thermal annealing of $PrBaMn_2O_6$ (O60A100) in air. The O60A70 and O60A50 samples appear to consist of two ferromagnetic phases: low temperature and high temperature ones. The as-prepared O30A00 and A-site ordered O60A00 samples have only one ferromagnetic phase (the so-called low temperature phase) with T_C up to $\sim$140 K. There is also one ferromagnetic phase (high temperature) with $T_C \approx 320$ K which appears at $\sim$250 K for A-site ordered O60A00. Upon thermal treatment of the O60A100 sample at 1300 °C in air there is a ferromagnetic component that appears at low temperature, similar to the case for the as-prepared O30A00 sample. This low temperature ferromagnet component is destroyed at around 180 K. In the process of the successive reoxidations in the temperature region 1100–1300 °C the high temperature phase disappears and the sample becomes the same as the parent $Pr_{0.50}Ba_{0.50}MnO_3$ sample.

The electrical resistivity and magnetoresistance versus temperature in a field of 9 kOe for some of the samples considered are presented in figure 5. All the samples treated in flowing argon and under high pressure show high resistivity (ρ) in comparison with the as-prepared $Pr_{0.50}Ba_{0.50}MnO_3$ (O30A00) sample. The latter has a resistivity of about 10 Ω cm, a metal–insulator (M–I) transition at $\sim$130 K and a peak of magnetoresistivity reaching $\sim$50% in a field of 9 kOe. The value of the resistivity in the so-called metallic state (at low temperature) is considerably higher than Mott's value for the maximal metallic resistivity. The peak of the magnetoresistivity being slightly below the Curie temperature is very typical for hole-doped manganites. For the A-site ordered $PrBaMn_2O_6$ (O60A100) sample the resistivity
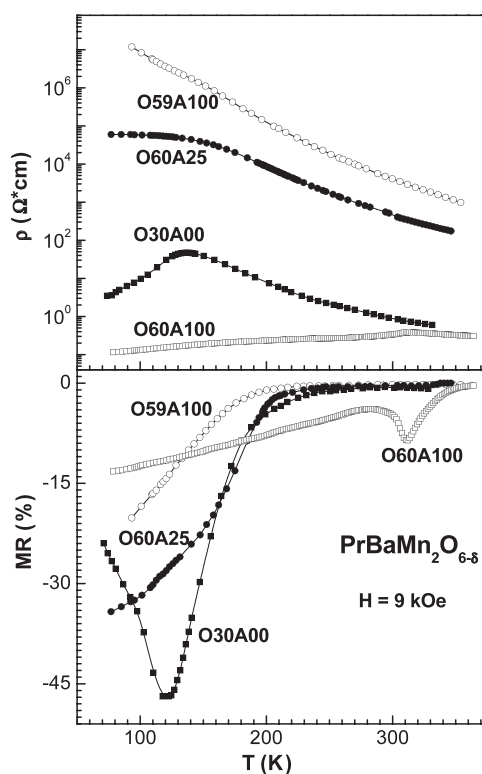
Figure 5. The electrical resistivity (upper panel) and magnetoresistance (lower panel) in a field of 9 kOe for the PrBaMn$_2$O$_{6-\delta}$ samples: O30A00 (full rectangles), O60A100 (open rectangles), O60A25 (full circles), O59A100 (open circles).

is $\sim10^{-1}$ Ω cm and in the magnetically ordered state it starts to decrease as temperature decreases. The temperature corresponding to the maximal resistivity value is slightly below the Curie point. Near T_C there is a maximum of the magnetoresistance ($\sim10\%$) observed, as in the case of classic magnetic semiconductors. A gradual magnetoresistance increase was observed as temperature was decreased, which is characteristic of conducting magnetic ceramics. This type of magnetoresistance is due to intergranular electrical transport. The resistivity of the reduced samples is about 10^7 Ω cm without any transitions down to liquid nitrogen temperatures. The reduced samples remain insulators throughout the region of investigation, 77–350 K. The magnetoresistance for all the reduced samples has no peak. For the PrBaMn$_2$O$_6$ (O60A25) sample treated under high pressure the magnetoresistance starts to develop at 180 K, where the long range ferromagnetic order appears. Around liquid nitrogen temperature the magnetoresistance reaches $\sim35\%$ in a field of 9 kOe.

A double-exchange mechanism was proposed by Zener and de Gennes to explain the metallic behaviour and ferromagnetic interactions in hole-doped perovskite manganites [4, 28]. The basic process in this mechanism is e$_g$ manganese electrons hopping from Mn^{3+} (t$_{2g}^3$e$_g^1$, $S = 2$) to Mn^{4+} (t$_{2g}^3$, $S = 3/2$) via the oxygen without changes of the spin orientation. Thereby, Mn^{4+} and Mn^{3+} ions change places. The t$_{2g}^3$ electrons are always localized (giving rise to a local spin of 3/2), but the e$_g$ electron, which is hybridized with the oxygen 2p one, can be either localized or itinerant. As a result, itinerant e$_g$ electrons align the local t$_{2g}^3$ spins ferromagnetically and cause the metallic behaviour.

According to our magnetization data we can assume that the as-prepared $Pr_{0.50}Ba_{0.50}MnO_3$ (O30A00) sample consists of either one canting antiferromagnetic or two (ferromagnetic and antiferromagnetic) collinear phases since the magnetic moment in a field of 9 kOe is less than the theoretically possible values. de Gennes [28] has suggested that non-collinear magnetic structure forms at concentrations intermediate between those of the antiferromagnetic and ferromagnetic states while the alkaline-earth ion content increases. However, neutron diffraction experiments in a magnetic field [29] and high resolution electronic microscopy results [30] were interpreted as favouring a mixed magnetic state. Therefore, we think that our as-prepared samples are ferromagnetic media with antiferromagnetic clusters, because the concentration boundary of the ferromagnetic–antiferromagnetic transition in the $Ln_{1-x}Ba_xMnO_3$ systems is very close to $x = 0.50$ [9].

Upon Pr/Ba ordering, the magnetization magnitude of the $PrBaMn_2O_6$ (O60A100) sample decreases but the magnetic ordering temperature increases to more than double, up to $\sim$320 K. The small magnetic moment in a field of 9 kOe is a result of the increase of the antiferromagnetic phase which arises below 200 K or an insufficient magnetic field value in which saturation is not reached. The increase of T_C is explained by the suppression of the mismatch effect.

The magnetic state of the $Ln_{1-x}A_xMnO_3$ (A = Ca, Sr, Ba) manganites is known to be determined by the $\langle r_A \rangle$ average radii of alkaline-earth and rare-earth ions as well as the σ^2 value of the cation size mismatch in the A sublattice:

$$\sigma^2 = \sum_{i=1}^{n} x_i r_i - \langle r_A \rangle^2 \tag{5}$$

where x_i is the part of the perovskite A sublattice filled by i-type cations (fractional occupancy), with the corresponding radius r_i, and n is the number of cations in the A sublattice. This discrepancy value (variance) characterizes a mismatch between alkaline-earth and rare-earth ionic radii [31].

For $K = Mn^{3+}/Mn^{4+}$ equal to 0.7:0.3, the maximum magnetic moment and Curie temperature are observed for manganites. If K is close to 1:1 the ferromagnetic state transforms into an antiferromagnetic one as the Mn^{4+} ion concentration increases. The less the average ionic radius of the A sublattice and the more the Ln^{3+} and A^{2+} ionic radius mismatch, the lower the magnetic ordering temperature, as a rule [32].

According to the empirical Goodenough–Kanamori rules for 180° indirect superexchange interactions, the closer the average $\langle Mn–O–Mn \rangle$ bond angle to 180°, the larger the exchange interaction value [33]. In the case of the orbitally disordered state, the sign of the exchange interaction can change from positive to negative as $\langle Mn–O–Mn \rangle$ angle decreases to below the critical point. Whereas the Pr^{3+} and Ba^{2+} ions are distributed randomly in the perovskite A sublattice, the local dispersion of the Mn–O–Mn angle value suppresses the exchange interaction value. Consequently the mismatch effect and A-site randomness weaken the ferromagnetic properties.

The ordering of cations in the A sublattice of the perovskite structure leads to enhancement of and translation symmetry in the arrangement of Mn–O–Mn bond angles as well as to a decrease of the Mn–O bond lengths and, as a consequence, to the suppression of the mismatch effect. Note that the ordering of the Mn–O–Mn bond angles and their enhancement can also lead to a sharp increase of the magnetic ordering temperature.

Upon reduction, the Mn^{4+} ions are converted into Mn^{3+} ions and the intensity of the exchange interactions should decrease. $Mn^{3+}–O–Mn^{3+}$ interactions in octahedral coordination are magnetically anisotropic in the orbital ordered phase (ferromagnetic in the [001] direction and antiferromagnetic in the others) and isotropic (ferromagnetic) in the orbital disordered one [33]. It is also known that the sign of the exchange interactions $Mn^{i+}–O–Mn^{j+}$ ($i, j = 3, 4$)

depends on the anion surroundings. In the case of fivefold coordination these interactions became antiferromagnetic [34, 35]. Taking these considerations into account, we assume that the PrBaMn$_2$O$_{6-\delta}$ (O59A100 and O56A100) samples contain antiferromagnetic Mn^{3+} (sixfold coordination)–O–Mn^{3+} (fivefold coordination) and Mn^{3+} (sixfold coordination)–O–Mn^{4+} (fivefold coordination) interactions.

Upon high pressure treatment the PrBaMn$_2$O$_{6-\delta}$ (O59A25) sample transforms into the inhomogeneous ferromagnetic state with $T_C = 180$ K. It is known that the hydrostatic pressure stabilizes the ferromagnetic state of the La$_{1-x}$A$_x$MnO$_3$ manganites [36]. The effect of hydrostatic pressure is to enhance the transfer integral through increase of the Mn–O–Mn angle. Possibly the bond angle of manganese interactions was reduced under the high pressure treatment. In our case the A-site randomness increases and consequently the ferromagnetic state is weakened. We underline that the effects of high pressure processing and applied hydrostatic pressure are completely reversible. For the PrBaMn$_2$O$_6$ (O60A70, O60A50 and O60A00) air annealed samples, similar magnetic behaviour is observed.

The resistivity of the polycrystalline samples is determined by two contributions: the contribution from the intragrain regions (grains) and the contribution from the intergrain regions (grain boundaries). The spin-polarized intergrain tunnelling in these compounds has been carefully studied and is known to depend on the grain size and the properties of the intergranular matter which constructs the intergrain barrier [37, 38]. Polycrystalline manganites usually show two distinct kinds of MR effects. One is pronounced near the magnetic ordering temperature (intragrain MR); the other is dominant at low temperature where the magnetization is substantial (intergrain MR) [39]. The ordering of cations in the A sublattice leads to increase of the transfer integral inside the grains through a change in the Mn–O–Mn angle. As a result the resistivity decreases. The resistivity of the reduced samples can be understood by assuming that it is determined by the Mn^{3+}/Mn^{4+} ratio and the presence of the oxygen bridges through which the electron hopping is realized. Hence the decrease of this ratio and the oxygen content leads to an increase of the resistivity.

4. Conclusion

The crystal structure, magnetization and electrotransport properties for the A-site ordered PrBaMn$_2$O$_{6-\delta}$ manganites after preparation under extreme conditions have been studied. The parent A-site ordered PrBaMn$_2$O$_6$ samples were prepared using a 'two-step' synthesis method from A-site disordered Pr$_{0.50}$Ba$_{0.50}$MnO$_3$ ones. The most significant structural feature of the A-site ordered manganites is that the MnO$_2$ sublattice is sandwiched by two kinds of rock-salt layers, PrO$_x$ and BaO. The oxygen-stoichiometric A-site ordered PrBaMn$_2$O$_6$ demonstrates a ferromagnetic metallic to paramagnetic insulating transition with the Curie point at about 320 K. These compounds are stable in air up to 1300 °C. The reduction of the A-site ordered PrBaMn$_2$O$_6$ samples leads to the appearance of an antiferromagnetic state with a Néel point at about 140 K, while the A-site order remains. Upon high pressure treatment the degree of A-site order decreases, which reduces T_C. The magnetotransport properties of the A-site ordered manganites treated under different conditions are discussed in terms of the manganese valence, oxygen content and degree of A-site order.

Acknowledgments

References

[1] Coey J M D, Viret M and von Molnár S 1999 *Adv. Phys.* **48** 167
[2] Tokura Y and Tomioka Y 1999 *J. Magn. Magn. Mater.* **200** 1
[3] Jonker G H and Van Santen J H 1950 *Physica* **16** 337
[4] Zener C 1951 *Phys. Rev.* **82** 403
[5] Troyanchuk I O, Trukhanov S V, Szymczak H, Przewoznik J and Bärner K 2001 *JETP* **93** 183
[6] Trukhanov S V 2003 *J. Mater. Chem.* **13** 347
[7] Trukhanov S V, Lobanovski L S, Bushinsky M V, Khomchenko V A, Pushkarev N V, Troyanchuk I O, Maignan A, Flahaut D, Szymczak H and Szymczak R 2004 *Eur. Phys. J.* B **42** 51
[8] Krupicka S, Marysko M, Jirak Z and Hejtmanek J 1999 *J. Magn. Magn. Mater.* **206** 45
[9] Troyanchuk I O, Khalyavin D D, Trukhanov S V and Szymczak H 1999 *J. Phys.: Condens. Matter* **11** 8707
[10] Millange F, Caignaert V, Domenges B, Raveau B and Suard E 1998 *Chem. Mater.* **10** 1974
[11] Troyanchuk I O, Trukhanov S V, Szymczak H and Baerner K 2000 *J. Phys.: Condens. Matter* **12** L155
[12] Hwang H Y, Cheong S W, Radaelli P G, Marezio M and Batlogg B 1995 *Phys. Rev. Lett.* **75** 914
[13] Nakajima T, Kageyama H and Ueda Y 2002 *J. Phys. Chem. Solids* **63** 913
[14] Trukhanov S V, Troyanchuk I O, Hervieu M, Szymczak H and Bärner K 2002 *Phys. Rev.* B **66** 184424
[15] Nakajima T, Kageyama H, Yoshizawa H and Ueda Y 2002 *J. Phys. Soc. Japan* **71** 2843
[16] Arima T, Akahoshi D, Oikawa K, Kamiyama T, Uchida M, Matsui Y and Tokura Y 2002 *Phys. Rev.* B **66** 140408
[17] Kageyama H, Nakajima T, Ichihara M, Ueda Y, Yoshizawa H and Ohoyama K 2003 *J. Phys. Soc. Japan* **72** 241
[18] Nakajima T, Kageyama H, Yoshizawa H, Ohoyama K and Ueda Y 2003 *J. Phys. Soc. Japan* **72** 3237
[19] Spooren J, Rumplecker A, Millange F and Walton R I 2003 *Chem. Mater.* **15** 1401
[20] Akahoshi D, Uchida M, Tomioka Y, Arima T, Matsui Y and Tokura Y 2003 *Phys. Rev. Lett.* **90** 177203
[21] Nakajima T, Yoshizawa H and Ueda Y 2004 *J. Phys. Soc. Japan* **73** 2283
[22] Spooren J, Walton R I and Millange F 2005 *J. Mater. Chem.* **15** 1542
[23] Nakajima T, Kageyama H and Ueda Y 2004 *J. Magn. Magn. Mater.* **272–276** 405
[24] Nakajima T and Ueda Y 2004 *J. Alloys Compounds* **383** 135
[25] Ueda Y and Nakajima T 2004 *J. Phys.: Condens. Matter* **16** S573
[26] Shannon R D 1976 *Acta Crystallogr.* **32** 751
[27] Troyanchuk I O, Khalyavin D D, Trukhanov S V, Chobot G N and Szymczak H 1999 *JETP Lett.* **70** 590
[28] de Gennes P-G 1960 *Phys. Rev.* **118** 141
[29] Wollan E O and Koehler W C 1955 *Phys. Rev.* **100** 545
[30] Moreo A, Yunoki S and Dagotto E 1999 *Science* **283** 2034
[31] Rodriguez-Martinez L M and Attfield J P 1998 *Phys. Rev.* B **58** 2426
[32] Mahesh R and Itoh M 1999 *Phys. Rev.* B **60** 2994
[33] Goodenough J B, Wold A, Arnot R J and Menyuk N 1961 *Phys. Rev.* **124** 373
[34] Trukhanov S V, Bushinsky M V, Troyanchuk I O and Szymczak H 2004 *JETP* **99** 756
[35] Trukhanov S V 2005 *JETP* **100** 95
[36] Moritomo Y, Asamitsu A and Tokura Y 1995 *Phys. Rev.* B **51** 914
[37] Zhang N, Ding W, Zhong W, Xing D and Du Y 1997 *Phys. Rev.* B **56** 8138
[38] Zhang N, Zhang S, Ding W P, Zhong W and Du Y W 1998 *Solid State Commun.* **107** 417
[39] Lee S, Hwang H Y, Shraiman B I, Ratcliff W D and Cheong S-W 1999 *Phys. Rev. Lett.* **82** 4508